Evidence for a fence that impedes the diffusion of phosphatidylinositol 4,5-bisphosphate out of the forming phagosomes of macrophages

Urszula Golebiewska[a,b], Jason G. Kay[c], Thomas Masters[d], Sergio Grinstein[c], Wonpil Im[e], Richard W. Pastor[f], Suzanne Scarlata[a], and Stuart McLaughlin[a,d]

[a]Department of Physiology and Biophysics, Stony Brook University, Stony Brook, NY 11794; [b]Department of Biological Sciences and Geology, Queensborough Community College, Bayside, NY 11364; [c]Program in Cell Biology, Hospital for Sick Children, Toronto, ON M5G 1X8 Canada; [d]Mechanobiology Institute, National University of Singapore, 117411 Singapore; [e]Department of Molecular Biosciences and Center for Bioinformatics, University of Kansas, Lawrence, KS 66047; [f]Laboratory of Computational Biology, National Heart, Lung and Blood Institute, National Institutes of Health, Bethesda, MD 20892

ABSTRACT **To account for the many functions of phosphatidylinositol 4,5-bisphosphate (PIP_2), several investigators have proposed that there are separate pools of PIP_2 in the plasma membrane. Recent experiments show the surface concentration of PIP_2 is indeed enhanced in regions where phagocytosis, exocytosis, and cell division occurs. Kinases that produce PIP_2 are also concentrated in these regions. However, how is the PIP_2 produced by these kinases prevented from diffusing rapidly away? First, proteins could act as "fences" around the perimeter of these regions. Second, some factor could markedly decrease the diffusion coefficient, D, of PIP_2 within these regions. We used fluorescence correlation spectroscopy (FCS) and fluorescence recovery after photobleaching (FRAP) to investigate these two possibilities in the forming phagosomes of macrophages injected with fluorescent PIP_2. FCS measurements show that PIP_2 diffuses rapidly (D ~ 1 $\mu m^2/s$) in both the forming phagosomes and unengaged plasma membrane. FRAP measurements show that the fluorescence from PIP_2 does not recover (>100 s) after photobleaching the entire forming phagosome but recovers rapidly (~10 s) in a comparable area of membrane outside the cup. These results (and similar data for a plasma membrane–anchored green fluorescent protein) support the hypothesis that a fence impedes the diffusion of PIP_2 into and out of forming phagosomes.**

Monitoring Editor
Thomas F.J. Martin
University of Wisconsin

Received: Feb 9, 2011
Revised: Jun 15, 2011
Accepted: Jul 20, 2011

INTRODUCTION

The lipid phosphatidylinositol 4,5-bisphosphate (PtdIns(4,5)P_2 or PIP_2) plays many roles in the plasma membrane of mammalian cells. For example, it is the source of three different second messengers. It also acts as a regulator or second messenger itself when it activates scores of ion channels, mediates both endocytosis and exocytosis, facilitates phagocytosis, and contributes to attaching the cytoskeleton to the membrane (Di Paolo and De Camilli, 2006). How does one lipid do so much? A number of investigators have proposed there must be separate pools of PIP_2 in the plasma membrane. For example, Hinchliffe *et al.* (1998) stated that if PIP_2 "does function as a second messenger in its own right … the existence of discrete, functionally distinct, independently regulated PtdIns(4,5)P_2 pools seems inescapable." There is some evidence for "functionally distinct pools" of PIP_2 in the plasma membrane of mast cells (Vasudevan *et al.*, 2009) and in caveolae (Fujita *et al.*, 2009). There is good evidence that spatially, as well as functionally, distinct pools of PIP_2 exist in three different mammalian cell types: specifically, the surface concentration of PIP_2 is enhanced significantly (approximately fivefold) in the vicinity of syntaxin clusters, where exocytosis occurs in neuronal cells (Aoyagi *et al.*, 2005; Milosevic *et al.*, 2005; James *et al.*, 2008); in the forming phagosomes of macrophages

This article was published online ahead of print in MBoC in Press (http://www.molbiolcell.org/cgi/doi/10.1091/mbc.E11-02-0114) on July 27, 2011.

Address correspondence to: Stuart McLaughlin (smclaughlin@notes.cc.sunysb.edu).

Abbreviations used: Bodipy-TMR-PIP_2, Bodipy–tetramethylrhodamine–phosphatidylinositol 4,5-bisphosphate-C16; $DiIC_{12}$, 1,1′-didodecyl-3,3,3′,3′-tetramethylindocarbocyanine perchlorate; FCS, fluorescence correlation spectroscopy; FRAP, fluorescence recovery after photobleaching; Lyso-PC, 1-arachidoyl-2-hydroxy-*sn*-glycero-3-phosphocholine; PIP_2, phosphatidylinositol 4,5-bisphosphate; PIP5Ks, phosphatidylinositol 4-phosphate 5-kinases; PM-GFP, green fluorescent protein–tagged N-terminal region of Lyn kinase; TopFluor-PIP_2, 1-oleoyl-2-{6-[4-(dipyrromethene boron difluoride)butanoyl]amin}hexanoyl-*sn*-glycero-3-phosphoinositol-4,5-bisphosphate.

(Botelho *et al.*, 2000; Scott *et al.*, 2005); and in the furrows of dividing fibroblasts (Emoto *et al.*, 2005; Field *et al.*, 2005). The kinases that produce PIP_2, mainly the phosphatidylinositol 4-phosphate 5-kinases (PIP5Ks)—which exist as α, β, and γ isoforms—are also concentrated in these three regions [for reviews of PIP5Ks see Weernink *et al.* (2004), Santarius *et al.* (2006), and Mao and Yin (2007)]. For example, Milosevic *et al.* (2005) observed colocalization of PIP5Kγ and green fluorescent protein (GFP)–PH-PLC-δ1, a probe for PIP_2, in 300-nm clusters localized to the region where exocytosis occurs in PC12 cells, extending the work of Wenk *et al.* (2001). Emoto *et al.* (2005) showed that PIP5Kβ accumulates at the cleavage furrow during cytokinesis. Doughman *et al.* (2003) discussed the evidence that PIP5Kα is recruited to the phagosomal cup upon stimulation with opsonized beads in macrophages; a recent study (Mao *et al.*, 2009) documented the unique roles of PIP5Kγ and PIP5Kα in receptor-mediated phagocytosis. Furthermore, the enhanced local concentration of PIP_2 in forming phagosomes is critical for phagocytosis; a kinase-dead PIP5Kα blocks both local accumulation of PIP_2 and phagocytosis (Coppolino *et al.*, 2002). Similarly, an inactive PIP5Kβ blocks both accumulation of PIP_2 at the furrow and cytokinesis (Emoto *et al.*, 2005).

Thus different isoforms of PIP5Ks are concentrated, presumably by specific protein–protein interactions, in forming phagosomes, furrows, and syntaxin clusters. These PIP5Ks enhance the local surface concentration of PIP_2 in these regions. However, how is the PIP_2 produced by these PIP5Ks prevented from diffusing rapidly away from the source? Diffusion of a lipid over short subcellular distances in a fluid membrane is an extremely rapid process: the diffusion equation predicts that a local production of PIP_2 will *not* result in a significant local build-up of PIP_2 unless there are fences around the perimeter that impede movement of PIP_2 or the diffusion coefficient of PIP_2 is severely reduced in these regions (McLaughlin *et al.*, 2002; Hilgemann, 2007). In contrast, diffusion of a lipid over 10-fold longer distances, corresponding to the diameter of a cell, is 100-fold slower because the diffusion time is proportional to the square of the distance; this allows PI3K enzymes localized to the leading edge of many chemotaxing cells to generate a significant gradient of the lipid PIP_3 in the plasma membrane, as reviewed elsewhere (Swaney *et al.*, 2010).

Specifically, the measured diffusion coefficients of PIP_2 in the inner leaflet of the plasma membrane of different cell types are all of order $D \sim 1\ \mu m^2/s$ (Golebiewska *et al.*, 2008). If the diffusion coefficient of PIP_2 in the forming phagosome has a similar value, the Einstein relation ($x^2 = 4Dt$) predicts that in $t = 1$ s the extra surface PIP_2 produced in the forming phagosome would diffuse a distance $x = 2$ μm, comparable to the radius of a moderately large phagosome. However, the forming phagosomes maintain an enhanced level of PIP_2, a process mediated by PIP5Ks, for ~100 s under some situations (Botelho *et al.*, 2000; Scott *et al.*, 2005). Then, prior to the final fission, the level of PIP_2 is significantly depressed, a process mediated by PLC-γ and PI3K (Swanson, 2008). The depressed level of PIP_2 and enhanced level of PIP_3 prior to scission are also maintained for ~100 s under some circumstances. How?

We envision two simple explanations for why the PIP_2 produced by the localized PIP5Ks does not diffuse away more rapidly than it can be produced. First, proteins could act as "fences" or "corrals" at the perimeter of the forming phagosomes. The fences would act as a barrier to impede the diffusion of PIP_2 out of the forming phagosomes, allowing the surface concentration of PIP_2 to rise upon activation of PIP5Ks within the fence. We refer to this as the "fence hypothesis." In yeast, septin filaments act as a fence/corral to limit the diffusion of membrane proteins (Faty *et al.*, 2002; Finger, 2005; McMurray and Thorner, 2009) and possibly PIP_2 (Garrenton *et al.*, 2010). The fence constituents in mammalian cells such as macrophages may include septin filaments and/or actin-associated proteins, as the actin cytoskeleton is swept away from the central base region of the forming phagosome and concentrates in a band at the perimeter (e.g., Swanson, 2008). Second, some factor(s) could decrease significantly (e.g., >10-fold) the diffusion coefficient of PIP_2 in the forming phagosomes or regions where syntaxin is clustered. For example, proteins with clusters of basic residues, such as syntaxin (Lam *et al.*, 2008; Williams *et al.*, 2009) and myristoylated alanine-rich protein kinase C substrate (MARCKS; Gambhir *et al.*, 2004), can bind PIP_2 rapidly and reversibly by a simple electrostatic mechanism (McLaughlin and Murray, 2005). Thus these proteins can act as buffers of PIP_2. Syntaxin is concentrated at regions where exocytosis occurs, and MARCKS is concentrated in forming phagosomes: if they were present at a sufficiently high local surface concentration to bind 90% (or 99%) of the PIP_2, a simple analysis shows that they would decrease the effective value of the diffusion coefficient 10-fold (or 100-fold; Golebiewska *et al.*, 2008). Alternatively, there could be a latticework of proteins throughout the forming phagosomes that force PIP_2 to move by a relatively slow "hop diffusion" mechanism, as postulated for the diffusion of proteins in the plasma membrane (Kusumi *et al.*, 2005, 2010). Alternatively, lipid domains such as cholesterol-enriched rafts (Lingwood and Simons, 2010) might impede diffusion of PIP_2. We refer collectively to these buffer/hop/raft mechanisms that might decrease the D of PIP_2 within the phagosomes as the "reduced–diffusion coefficient hypothesis."

To distinguish between the fence and the reduced–diffusion coefficient hypotheses, we measured directly the diffusion coefficient of fluorescent PIP_2 in the forming phagosomes of macrophages and in the bulk plasma membrane outside the phagosomal cup. The process of phagocytosis in macrophages is reviewed elsewhere (Cougoule *et al.*, 2004; Stuart and Ezekowitz, 2005; Yeung *et al.*, 2006; Swanson, 2008): a major advantage of using this system to test whether PIP_2 fences exist is that macrophages will engulf large-diameter (8 μm) beads, which facilitates diffusion measurements in the forming phagosome. Specifically, we microinjected micelles containing fluorescent PIP_2 into macrophages and measured the diffusion coefficient of individual PIP_2 molecules that incorporated into the plasma membrane by using fluorescence correlation spectroscopy (FCS). To test the fence hypothesis more directly, we photobleached the PIP_2 within the forming phagosome. We reasoned that if a PIP_2 fence surrounds the forming phagosome, the fluorescence should not recover. We also reasoned that if a fence prevents the diffusion of PIP_2 out of the forming phagosome, it should also prevent the diffusion of a larger peripheral protein. Thus we obtained FCS and fluorescence recovery after photobleaching (FRAP) data on a GFP construct anchored to the plasma membrane through two acyl chains (GFP-tagged N-terminal region of Lyn kinase [PM-GFP]).

RESULTS

The level of PIP_2 in the forming phagosomes of J774a.1 macrophages first increases and then decreases

We used murine macrophages of the J774 line to study PIP_2 diffusion during phagocytosis. Although a biphasic change in PIP_2 during phagocytosis was demonstrated earlier in another line of murine macrophages, RAW 264.7 (Botelho *et al.*, 2000; Scott *et al.*, 2005), it was important to validate the occurrence of similar changes in J774 cells. As before, GFP-tagged PH domain from PLC-δ1 was used to monitor PIP_2 in live cells. As shown in Supplemental Figure S1, the fluorescence of the probe first increases and then

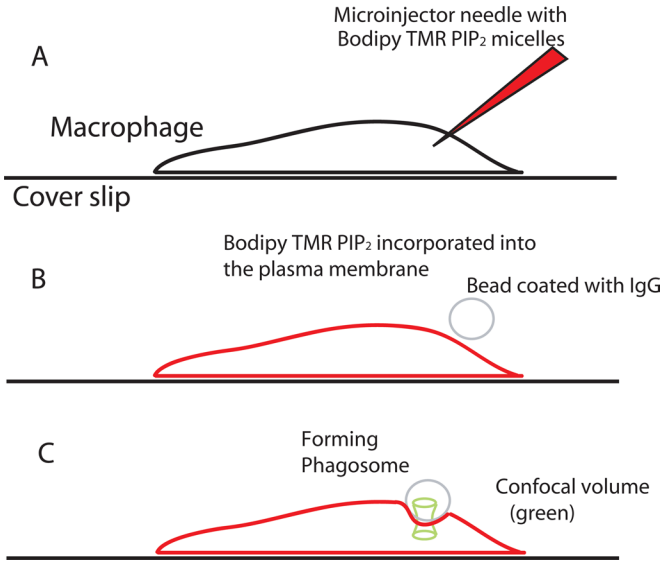

FIGURE 1: Methods used to study the diffusion of fluorescent PIP_2 in the forming phagosomes of macrophages. (A) Cartoon showing a J774a.1 macrophage and adjacent microinjector needle loaded with micelles containing Bodipy-TMR-PIP_2. (B) After microinjection, monomers of fluorescent PIP_2 incorporate rapidly into the inner leaflet of the plasma membrane, which is now colored red. The cell is then exposed to 8-μm-diameter latex beads coated with human IgG. One bead, colored gray, is shown in the process of landing on top of the cell. (C) The cell begins to ingest the bead by the process of Fcγ receptor–mediated phagocytosis. The laser focus (green hourglass) is positioned on the top membrane in the middle of the forming phagosome to obtain the FCS data from fluorescent PIP_2 molecules diffusing into and out of this area.

decreases in the forming phagosome as the J744 cell engulfs immunoglobulin G (IgG)–coated latex beads. The increase in PLC-δ1PH, interpreted as an increased surface density of PIP_2 at the phagosomal cup, is presumably due to localized, activated PIP5Ks; the decrease presumably results from cleavage to diacylglycerol by activated PLC-γ and conversion to PIP_3 by activated PI3K, as discussed in detail elsewhere (Botelho *et al.*, 2000; Marshall *et al.*, 2001; Coppolino *et al.*, 2002; Scott *et al.*, 2005; Swanson, 2008).

PIP_2 diffuses rapidly on the inner leaflet of the plasma membrane both inside and outside of the cup

How can the local production of PIP_2 by PIP5Ks concentrated in the forming phagosome elevate the local level of PIP_2? Specifically, if the diffusion coefficient of PIP_2 in the plasma membrane is ~1 $\mu m^2/s$, then McLaughlin *et al.* (2002) argue the local surface concentration of PIP_2 "is unlikely to change significantly in response to enhanced local synthesis of PIP_2 by a PIP kinase. Put simply, PIP_2 will diffuse away faster than it can be produced." Detailed calculations by Hilgemann (2007) suggest the diffusion coefficient would have to be greatly reduced (>10-fold) to account for the measured local accumulation of PIP_2. Thus we measured directly the diffusion coefficient of PIP_2 in the forming phagosome (Figure 1).

As shown in Figure 1A, we microinjected mixed micelles (1-arachidoyl-2-hydroxy-*sn*-glycero-3-phosphocholine [Lyso-PC] + Bodipy–tetramethylrhodamine–PtdIns(4,5)P2-C16 [Bodipy-TMR-PIP_2]) into macrophages. As with other cells, the mixed micelles deliver the fluorescent PIP_2 to the inner leaflet of the plasma membrane, which is shown red in Figure 1B (Golebiewska *et al.*, 2008). In Figure 1B, an 8-μm-diameter, IgG-coated bead is shown landing on the top of the cell. Figure 1C illustrates that the cell begins to ingest the IgG-coated beads that contact them by the process of Fcγ receptor–mediated phagocytosis (Swanson, 2008).

The fluorescence is then scanned through the cell, from bottom to top, and the location of the upper plasma membrane that defines the forming phagosome is determined. As shown in Figure 1C, the waist of the confocal beam is positioned over the upper membrane, in the cup of the forming phagosome, and the fluorescence is recorded as a function of time.

Figure 2A shows the results from a scan of the fluorescence through the cell. The peaks, separated by ~3 μm, represent the lower and upper plasma membrane. The confocal volume is focused on the upper membrane, the fluorescence is recorded as a function of time, typically for 10-s periods, and the autocorrelation function is calculated by the Zeiss program. Figure 2B illustrates a typical autocorrelation function of Bodipy-TMR-PIP_2 in the plasma membrane of the same forming phagosome shown in Figure 2A. These measurements were taken early in formation of the cup, where independent measurements show that the level of PIP_2 has increased (see Supplemental Figure S1). Equation 1 (see *FCS measurements*, *Materials and Methods*; Figure 2B, red curve) was fitted to the experimental autocorrelation curve (Figure 2B, black line). The correlation time—the midpoint of the curve—is the average time an individual fluorescent PIP_2 spends in the confocal area of radius 0.22 μm. The correlation time τ_d was 24 ms for this example. The diffusion coefficient, D, of the fluorescent PIP_2 in the forming phagosomes was calculated from Eq. 2 (*FCS measurements*, *Materials and Methods*). The measurements were repeated on an identical area of the plasma membrane located outside of the cup/forming phagosome. Figure 2C shows that the average value of D within the forming phagosome (red square; ~0.9 $\mu m^2/s$) does not differ significantly from the average value in the unengaged plasma membrane outside of the forming phagosome (cyan square; ~1.1 $\mu m^2/s$). It is also the same as the average value of D in the inner leaflet of the plasma membranes of six other cell types (e.g., Cos1, HEK293); data from Rat1 fibroblasts (green square; ~1 $\mu m^2/s$) are from Golebiewska *et al.* (2008).

To account for the ability of the PIP5Ks to produce an enhanced local concentration of PIP_2, the diffusion coefficient of PIP_2 should be reduced >10-fold within the cup (Hilgemann, 2007). It is not (Figure 2C). In fact, it diffuses equally rapidly within and outside of the cup. Thus we conclude that the experimental results summarized in Figure 2C rule out the reduced–diffusion coefficient hypothesis. We therefore shift our attention to the alternative fence hypothesis.

As predicted by the fence hypothesis, the signal from fluorescent PIP_2 diffusing in the inner leaflet of the plasma membrane of a phagosomal cup does not recover after photobleaching the entire cup

To test more directly the hypothesis that there is a fence/corral that limits the diffusion of PIP_2 across the perimeter of the forming phagosome, we carried out FRAP measurements on 1-oleoyl-2-{6-[4-(dipyrromethene boron difluoride)butanoyl]amin}hexanoyl-*sn*-glycero-3-phosphoinositol-4,5-bisphosphate (TopFluor-PIP_2) in the phagosomal cups of J774 macrophages. TopFluor-PIP_2 bleaches more easily than Bodipy-TMR-PIP_2 and is thus more suitable for FRAP measurements. We microinjected fluorescent PIP_2 into the cytoplasm of cells in the form of mixed micelles (see *Materials and Methods*) and observed, as expected, that TopFluor-PIP_2 rapidly incorporated into the plasma membrane of cells; a fraction of this lipid also remained in cytosolic compartments (Figure 3).

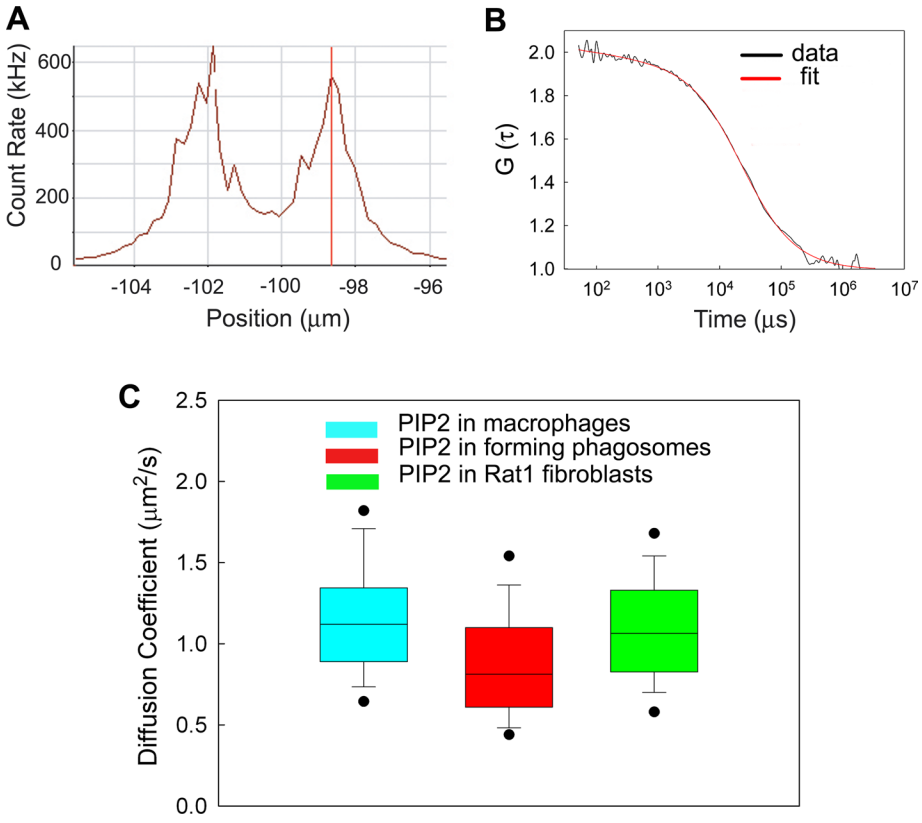

FIGURE 2: FCS measurements of PIP_2 diffusion in the phagosomal cups of macrophages. (A) Fluorescence intensity scan in the z-direction through the center of the phagosomal cup region of a J774a.1 macrophage. The cell was injected with arachidoyl–Lyso-PC/Bodipy-TMR-PIP_2 micelles prior to addition of beads. The peaks correspond to the positions of the plasma membrane. We focused on the top membrane to perform FCS measurements. T = 25°C. (B) Autocorrelation function, G(τ), of Bodipy-TMR-PIP_2 diffusing in the forming phagosomal cup of the J774a.1 macrophage shown in A. The red curve represents the fit of Eq. 1, the equation for free Brownian diffusion in two dimensions, to the data. The average residency or correlation time (approximate midpoint of curve) is 24 ms for this example. (C) Average diffusion coefficients of Bodipy-TMR-PIP_2 in the plasma membrane of macrophages (cyan), in the forming phagosomal cups of macrophages (red), and in the plasma membrane of a different cell, the Rat1 fibroblast (green). The dots represent the 5th and 95th percentiles, the vertical bars represent the standard deviations, and the heights of the boxes represent the standard errors. The diffusion coefficient of PIP_2 in the phagosomal cup (red; 0.9 $\mu m^2/s$) is not significantly lower than in the area outside the cup (cyan; 1.1 $\mu m^2/s$).

We then added 8-μm-diameter latex beads coated with human IgG to the solution bathing the cells. The microinjected cells initiated the process of phagocytosis. For FRAP measurements, we selected cells in early stages of phagocytosis (plasma membrane envelops ~10–20% of the bead) using transmitted light and the LSM module. Figure 3 shows an example of one of these FRAP measurements. We recorded three images prior to the bleach (Figure 3A), bleached the TopFluor-PIP_2 in the phagosomal cup within 1.5 s (Figure 3B), and monitored fluorescence for ~100 s after the bleach (Figure 3C). Fluorescence was recorded in the region indicated by the dashed white lines. As shown in Figure 3D, the level of fluorescence in this cell did not recover significantly. The simplest interpretation of this result is that a fence/corral, presumably of protein origin, impedes diffusion of fluorescent PIP_2 into and out of the phagosomal cup during its formation.

As a control, we made FRAP measurements on TopFluor-PIP_2 in the plasma membrane of quiescent macrophages. As shown in Figure 3E, the fluorescence signal recovered rapidly (recovery half-time was ~10 s for a region of radius ~3 μm) and fully (to 95% of corrected fluorescence in unbleached portion of membrane), consonant with a relatively unconstrained diffusion of fluorescent PIP_2 into the bleached area. The data in Figure 3E represent one typical example of these control measurements; see Supplemental Section 2 for more details).

A similar FRAP experiment with the fluorescent lipid 1,1′-didodecyl-3,3,3′,3′-tetramethylindocarbocyanine perchlorate (with 12 C chains [$DiIC_{12}$]) shows that the lack of recovery in Figure 3D with PIP_2 is not due to technical problems in monitoring fluorescence recovery in the vicinity of a bead during phagocytosis. When we bleached the fluorescence due to DiI in a forming phagosome, the fluorescence recovered fully (to >80% of the initial value) and rapidly (with a time constant of ~10 s), as shown in Supplemental Figure S2. This result was expected: DiI can rapidly flip-flop across the membrane (Melikyan *et al.*, 1996). The evidence suggests that there is no barrier to the diffusion of DiI on the outer leaflet (or GPI-GFP; see Supplemental Section 3).

FCS and FRAP measurements on PM-GFP suggest that its diffusion into the forming phagosome is, like that of PIP_2, limited by a fence

We made FCS measurements on PM-GFP expressed in macrophages to measure how rapidly this model peripheral protein diffuses in both the cup of the forming phagosome in RAW macrophages and in the membrane outside the cup. The construct tags the N-terminal 10 residues of the Src family kinase Lyn with GFP. Thus the construct should be myristoylated as well as palmitoylated in the RAW macrophages and should be targeted to the plasma membrane by the same mechanism as Lyn. We observed that PM-GFP, which is found mainly on the plasma membrane, diffuses rapidly both inside and outside of the phagosomal cup. Specifically, the measured correlation times (average values of 32 ms inside the cup and 27 ms outside the cup) correspond to a D ~ 0.7 ± 0.4 $\mu m^2/s$ (n = 28 ± SD) within the cup and 0.9 ± 0.5 $\mu m^2/s$ (n = 25 ± SD) outside the cup. Hammond *et al.* (2009) reported a very similar value for the D of PM-YFP in HEK cells (0.79 $\mu m^2/s$) using FRAP. (We note in passing that PM-GFP diffuses almost as rapidly as the lipid PIP_2: in both cases D is ~1 $\mu m^2/s$. The simplest interpretation is that the predominant component of the diffusional drag on PM-GFP is exerted by the two acyl chains, which insert into the hydrophobic—and relatively high viscosity—interior of the plasma membrane. Although GFP is larger (a cylinder ~3 nm in diameter by 4 nm in height) than the head group of PIP_2 (~1 nm diameter), the GFP moiety presumably exerts a minimal effect on D because it is diffusing in a medium of relatively low viscosity.)

If a protein fence impedes the diffusion of PIP_2 into and out of the forming phagosome, we expect that it will also impede the movement of the larger PM-GFP. Figure 4 shows that when we photobleached the PM-GFP within a phagocytic cup the

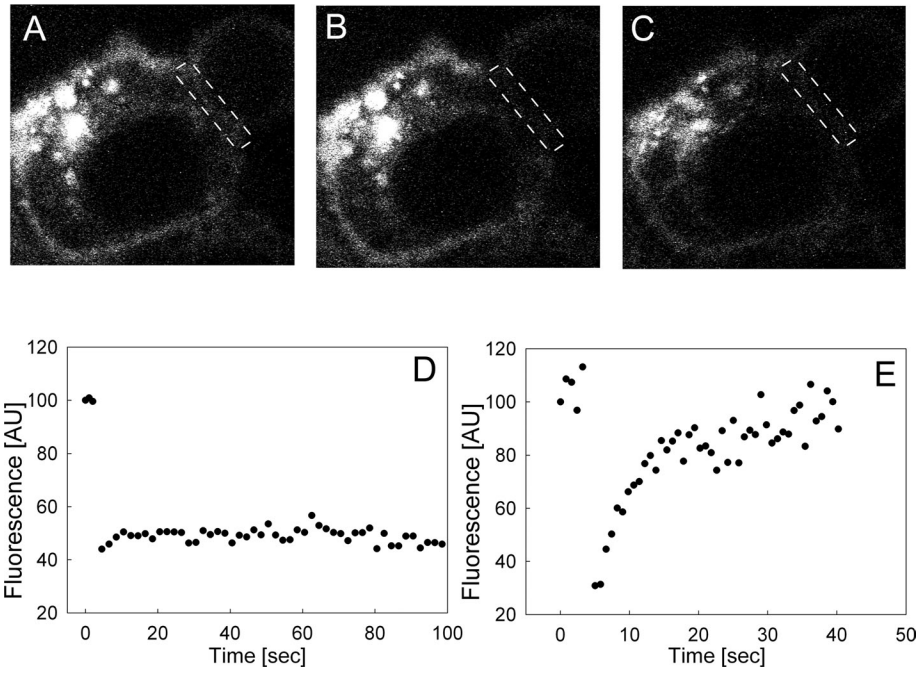

FIGURE 3: FRAP measurements on fluorescent PIP_2 are consistent with a fence around the forming phagosome. FRAP measurements of TopFluor-PIP_2 in the phagosomal cup of a J774 cell. (A) Cell injected with TopFluor-PIP_2 prior to the bleach. The rectangle of dashed white lines indicates the region of the phagosomal cup we bleached. (B) The same cell immediately after a 1.5-s bleach. (C) The same cell ~100 s after the bleach. (D) Time trace of average fluorescence intensity per pixel in the region of the forming phagosome indicated by the dashed lines. T = 25°C. Result representative of experiments on nine different cells. (E) Control experiment that shows that the fluorescence due to TopFluor-PIP_2 recovers rapidly (time constant ~10 s) and fully when we bleach a similar area in an unstimulated J774 macrophage (or in a region outside of the cup).

fluorescence recovered (with a time constant of 15 s) to a maximum value of only 20% within 100 s (Figure 4, A, top, Cup; and B, black squares). However, when we subsequently bleached a comparable area of membrane (radius ~2 μm) in the same cell in a region outside the cup, the fluorescence recovered more fully to ~70% of the initial value (Figure 4, A, bottom, PM; and B, open circles). Thus results with this membrane-anchored probe recapitulate the results we obtained with PIP_2: the fluorescence recovers only partially within the cup but more fully outside the cup. This result provides additional support for the existence of a corral/fence around the perimeter of the forming phagosome. (The recovery of ~70% illustrated in Figure 4B is typical of 20 measurements for the PM outside the cup. In two cases we prebleached the area: this resulted in a recovery of ~100% for the second photobleach, as shown in Supplemental Figure S3.)

We interpret the FCS and FRAP measurements reported here differently than the similar FRAP measurements on PM-GFP reported previously for macrophages by Corbett-Nelson *et al.* (2006), as discussed in Supplemental Section 3. The results shown in Figures 4 and Supplemental Figure S3 are in good accord with those obtained by Schmidt and Nichols (2004), who reported a barrier for diffusion of PM-GFP (aka Lyn-GFP) at the cleavage furrow of dividing mammalian cells.

Diffusion of molecules is reduced, but only slightly, in actin-rich areas at the periphery of the forming phagosome

As discussed in reviews (e.g., Swanson, 2008), actin accumulates at sites of phagocytosis and is particularly abundant at the tips of advancing pseudopods (Figure 5A). We therefore considered the possibility that actin-rich structures constitute a diffusional barrier that confines lipids and proteins within the forming phagosomal cup. For these experiments the mobility of fluorescent membrane components was assessed by FRAP. To stabilize the focal plane during the course of the measurements, we used a model of frustrated phagocytosis in which the ligand, IgG, is attached to the surface of a coverslip. The cells are allowed to settle by gravity onto the coated surface, whereupon they extend an aborted phagocytic cup. The development of this process is illustrated in Figure 5B, where the fluorescence of cells transfected with mCherry-actin is monitored at the plane of contact. Actin forms a distinct rim around the periphery of the extending cup, replicating the behavior observed in Figure 5A. To assess whether the actin rim serves as a diffusional barrier, we cotransfected cells with mCherry-actin and with GFP-tagged membrane-associated probes. These included either lipid-anchored GFP (the diacylated PM-GFP or the farnesylated and palmitoylated GFP-tH) and a GFP-tagged protein that spans the membrane once (GT46-GFP). The mobility of these probes was assessed during the course of frustrated phagocytosis in two areas: near the center, where actin is largely depleted, and near the edge, where the actin rim is most prominent (Figure 5C). For comparison, the diffusion of the probes was also measured in the ventral membrane of cells that were grown on coverslips not coated with IgG (designated as "control"). Figure 5D summarizes the results of these experiments. The two probes attached to the inner leaflet of the plasma membrane (PM-GFP and GFP-tH) behaved in a similar manner: their diffusion coefficient in the center of the frustrated phagosome was not retarded compared with that in control membranes, whereas diffusion was modestly retarded in the actin-rich region of the membrane. In contrast, the mobility of an exofacial probe—glycosylphosphoinositol-linked GFP (GPI-GFP)—was not different in the different regions of the forming phagosome.

Whereas diffusion of the transmembrane or inner leaflet–associated probes was reduced by actin and/or actin-associated components, the observed changes in mobility are comparatively modest (less than twofold; Figure 5D). Thus actin filaments are unlikely to account for the lack of recovery after photobleaching noted in the cup region for PM-GFP (Figure 4).

Actin filaments by themselves are unlikely to constitute the PIP_2 fence

Although most of the actin filaments in the cortical cytoskeleton are probably located some distance (>2 nm) from the bilayer leaflet, electron tomography measurements suggest that a fraction of the actin filaments may be located in close proximity (<1 nm) to the plasma membrane (Morone *et al.*, 2006). Actin has a net negative charge, and the electrostatic potential adjacent to most of the filament is negative (Supplemental Figure S4). Given that PIP_2 is also negatively charged (valence of −4 at pH 7 [McLaughlin *et al.*, 2002]),

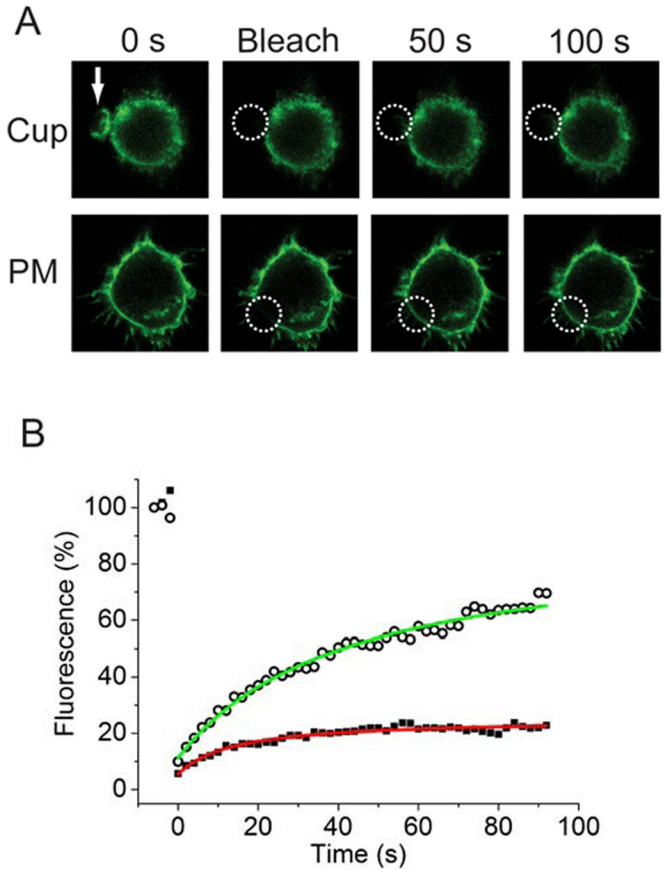

FIGURE 4: Fluorescence due to PM-GFP within a phagocytic cup does not recover after photobleaching. RAW 264.7 macrophages transfected with a GFP construct that is targeted to the plasma membrane (PM-GFP) were allowed to engage 8-μm-diameter opsonized beads at 37°C (A, top; bead location indicated by white arrow). (A) Top, bleach of cup. PM-GFP within the cup was bleached, and selected images are shown from the time course of recovery. The frame "bleach" indicates the first frame after execution of the bleach cycle (~2-s duration). Note that the fluorescence recovers only slightly in 100 s. Bottom, bleach of plasma membrane (PM) outside of the cup. Note that the fluorescence does recover after bleach of a similar area in the same cell. The white dashed circles indicate the bleached areas in both cases. (B) Fluorescence recovery curves for the two experiments shown in A. Inside the cup (filled black squares, red line) the fluorescence recovers only 20%; outside of the cup (open circles, green line) the fluorescence recovers 70%. The figure is representative of five similar results where the entire cup was bleached.

actin filaments in close proximity (<1 nm, approximately a Debye length) to the inner leaflet might be expected to reduce its diffusion, that is, act as electrostatic fences. To set a plausible upper limit on this effect, Langevin dynamics computer simulations of PIP_2/actin model systems were carried out on a range of geometries and salt concentrations. The simulations indicate that even if actin filaments were within 0.5 nm of the membrane surface, PIP_2 diffusion would be reduced by only ~20% when the salt concentration is 150 mM. The explanation for the lack of a large effect is simple. Although an actin filament has a net negative charge, it also has a band of basic (positively charged) residues that spiral around the actin filament much like the blue ribbon spirals around a barber pole (Supplemental Figure S4). These basic residues (in the spiral) provide electrostatic gaps, which coincide with geometric gaps, in the putative actin fence rail and allow PIP_2 to escape (Supplemental Figure S4).

DISCUSSION

FCS and FRAP measurements on fluorescent PIP_2 and PM-GFP provide evidence for a fence that limits diffusion

The surface concentration of PIP_2 first increases and then decreases in the phagosomal cups of J774 macrophages (Supplemental Figure S1), as previously observed in RAW macrophages (Scott *et al.*, 2005). Our FCS measurements show directly that the diffusion coefficient of PIP_2, D, has similar high values both inside and outside of the phagosomal cup (Figure 2, D ~ 1 $\mu m^2/s$). This result falsifies the low–diffusion coefficient hypothesis. Instead, the data are consistent with the alternative fence hypothesis: molecules located at the perimeter of the phagosomal cup impede the diffusion of PIP_2 into and out of the cup.

The fluorescence associated with PIP_2 does not fully recover within 100 s when we bleach the area of the cup but does rapidly recover when we bleach an area outside of the cup (Figure 3): this FRAP result supports the hypothesis there is a fence at the perimeter or lip of the cup. Similar FCS and FRAP measurements on PM-GFP show the fence also limits the diffusion of this construct into and out of the forming phagosome (Figure 4 and Supplemental Figure S3).

The collar of cortical actin filaments apparent at the leading edge of the forming phagosome (Figure 5A) is associated with only a moderate decrease in the diffusion coefficients of model peripheral proteins such as PM-GFP (Figure 5D); the decrease (less than twofold) is not sufficient to account for the lack of recovery after photobleaching observed with PM-GFP in Figure 4 and Supplemental Figure S3. Furthermore, our theoretical calculations suggest that actin filaments alone are unlikely to exert a sufficient barrier to account for the limited diffusion of PIP_2 out of a forming phagosome (Supplemental Figure S4).

The relatively sharp boundary between the enhanced level of PIP_2 and PIP_3 in the forming phagosome and the lower levels of PIP_2 and PIP_3 in the contiguous extraphagosomal membrane (e.g., Supplemental Figure S1) also support the fence hypothesis. What proteins might act as fences?

Nature of the fence

Septin filaments, which are described in detail elsewhere (Hall *et al.*, 2008; McMurray and Thorner, 2009; Oh and Bi, 2011; Estey *et al.*, 2011), can act as diffusional barriers in yeast. Their structure is known: specifically, six human (or eight yeast) septin monomers join together to form hetero-oligomeric rods (Sirajuddin et al., 2007; see also Supplemental Figure S5). The rods join together to form filaments: in yeast the filaments separate mother cell from daughter bud. FRAP measurements show that fluorescently tagged proteins diffusing freely in the daughter buds do not cross the barrier to the mother cell until the temperature is raised and the septin structure is disrupted (Barral *et al.*, 2000; Takizawa *et al.*, 2000), as reviewed elsewhere in detail (Faty *et al.*, 2002; Finger, 2005). Less direct evidence suggests that the split septin rings at the neck of budding yeast may allow PIP_2 to accumulate in this membrane microdomain (Yoshida *et al.*, 2009; Garrenton *et al.*, 2010). Garrenton *et al.* (2010) also showed that PIP_2 accumulates in the protrusions of yeast responding to pheromones (shmoo formation); of importance, they observed a septin lattice network at the boundary of the PIP_2-rich protrusion. This region of enhanced PIP_2 concentration lasts ~100 min, which, as they note, requires a diffusion barrier. In Supplemental Section 5 we consider how mammalian septin filaments could bind to the inner leaflet of the plasma membrane.

Septins appear in the right place at the right time to be implicated in the formation of PIP_2 fences in macrophages; they appear

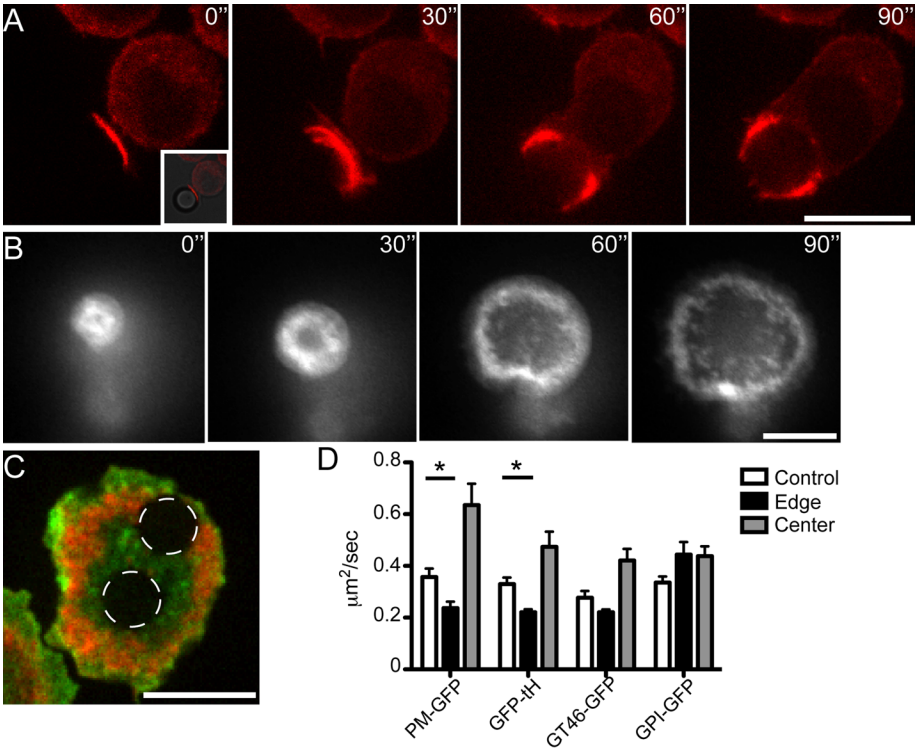

FIGURE 5: Diffusion of proteins in the actin-rich region at the perimeter of the forming phagosome. (A) RAW macrophages with stable expression of mCherry-actin were allowed to phagocytose 8-μm-diameter latex beads opsonized with human IgG. A time course of actin dynamics during the phagocytosis is shown. Following initial contact and nascent phagosome formation (0˝), F-actin continues to surround the bead (30˝). When the F-actin reaches around ~1/2 the bead, clearance of the F-actin occurs at the base of the cup (60˝). The cleared area continues to grow as the bead is engulfed by the advancing F-actin (90˝). Scale bar, 10 μm. T = 37°C. (B) Time course of GFP-actin dynamics during frustrated phagocytosis. Stable GFP/actin–expressing RAW macrophages were "parachuted" onto a coated coverslip. The coverslip was coated with BSA, followed by opsonization with mouse anti-BSA monoclonal antibody. Initial contact with coverslip is shown (0˝), followed by a time course of the macrophage forming a phagocytic "cup" with a thick F-actin ring. The ring advances along the coverslip, with clearing of F-actin from the center of the "cup" (30–90˝). The cell eventually becomes "frustrated" and the cup disassembles (not shown). Dynamics of F-actin ring formation and clearance are similar to those during phagocytosis of a particle as shown in A. Scale bar, 10 μm. (C) Example of photobleaching performed for FRAP experiments with macrophage expressing both mCherry-actin (red) and PM-GFP (green) following parachuting of cells onto opsonized coverslips and formation of the frustrated cup. Spinning disk confocal image of cell after photobleaching of a 3-μm-diameter circle (white dashed lines) inside an area cleared of F-actin, as well as 3-μm-diameter area in the F-actin ring of the frustrated cup. Scale bar, 5 μm. (D) Diffusion coefficients determined by FRAP for tested constructs. FRAP areas were either within the F-actin–cleared frustrated cup (Center) or within the strong F-actin ring of the frustrated cup (Edge). FRAP was also done on control cells grown on coverslips without opsonin present (Control). PM-GFP is the N-tail 10 residues of Lyn (myristoylated and palmitoylated) fused to GFP. tH-Ras-GFP is the minimal membrane targeting sequence from H-Ras (palmitoylated and farnesylated) fused to GFP. GT46-GFP is a nonraft transmembrane chimera fused to GFP, and GPI-GFP is an outer leaflet glycosylphosphatidylinositol-anchored GFP fusion protein. Intracellular lipid-anchored probes are significantly slowed in the F-actin ring of the frustrated cup, but the effect is small (less than twofold). The recovery rate of the GPI probe on outer membrane leaflet is not affected. Asterisk indicates statistical difference with $p < 0.05$. Error bars indicate SEM (of n = 4–16 measurements per condition).

in the forming phagosomes when the PIP_2 level in the forming phagosome starts to increase, and procedures that move septins off the membrane also inhibit the final step of phagocytosis (Huang *et al.*, 2008). Septin filaments are also present near syntaxin clusters in neuronal cells (Froese and Trimble, 2008) and in the furrows of dividing mammalian cells (Schmidt and Nicholls, 2004): thus septin filaments are candidates to act as PIP_2 fences at these locations.

Importance of the fence for phagocytosis

Several lines of evidence suggest that local changes in the level of the phosphoinositides PIP_2 and PIP_3 are important for phagocytosis (Araki *et al.*, 1996; Coppolino *et al.*, 2002; Swanson, 2008). However, it is not fully understood why PIP_2 is important (Swanson, 2008). A reasonable speculation is that an increase in the local level of PIP_2 may be required to enhance attachment of the actin-rich cytoskeleton to the membrane; a decrease in the local level of PIP_2 may facilitate cytoskeletal dissociation from the membrane and scission of the phagosome (Scott *et al.*, 2005). A similar dependence of membrane–cytoskeleton interactions on the global level of PIP_2 has been observed in a number of cells (Raucher *et al.*, 2000). Whatever the mechanism(s) by which PIP_2 acts, it is clear that because PIP_2 diffuses rapidly in the plasma membrane, a fence is required to maintain an enhanced level of PIP_2 synthesized by local PIP5Ks.

In conclusion, we note that there is much indirect evidence for separate pools of PIP_2 in the plasma membrane. Our FCS (Figure 2) and FRAP (Figure 3) measurements on fluorescent PIP_2 in the plasma membrane of macrophages provide direct support for the hypothesis that there is a PIP_2 fence around the forming phagosomes in macrophages: the fence impedes the diffusion of PIP_2 into and out of the cup. This fence allows the surface concentration of PIP_2 in the cup to first increase (due to the action of PIP5Ks) and then decrease (due to the action of PLC, PI3K) during phagocytosis. Previous work shows these changes in PIP_2 in the forming phagosome are functionally important for phagocytosis. The nature of the fence is unknown, but septin filaments are a viable candidate.

MATERIALS AND METHODS

Materials

Bodipy-TMR-PIP_2 was purchased from Echelon Bioscience (Salt Lake City, UT). The chemical structure of this lipid is illustrated in Gambhir *et al.* (2004). TopFluor-PI(4,5)P_2 was purchased from Avanti Polar Lipids (Alabaster, AL). DilC_{12} was purchased from Invitrogen (Carlsbad, CA). Arachidoyl Lyso-PC was purchased from Avanti Polar Lipids. Rhodamine B and human IgG were from Sigma-Aldrich (St. Louis, MO). The 8-μm latex beads were from Bangs Labs (Fishers, IN). Glass capillaries, thin walled with filament inner diameter 1.0 mm, were purchased from World Precision Instruments (Sarasota, FL). Needles were pulled on a Flaming Brown micropipette puller, model P.80/PC, Sutter

Instrument (Novato, CA). The 35-mm glass-bottom dishes were purchased from MatTek Corporation (Ashland, MA).

Cell culture

J774A.1 macrophages were purchased from the American Type Culture Collection (ATCC; Manassas, VA). Cells were maintained at 37°C with 5% CO_2 in DMEM supplemented with 10% fetal bovine serum (FBS), 50 U/ml penicillin, 50 µg/ml streptomycin sulfate, and sodium pyruvate. J774A.1 cells used in the examination of PIP_2 and PIP_3 levels with GFP-tagged probes were maintained at 37°C with 5% CO_2 in DMEM with 1.5 g/l sodium bicarbonate from Wisent (St. Bruno, QC, Canada) supplemented with 10% FBS. RAW 264.7 cells used for the actin localization and frustrated phagocytosis experiments were from ATCC and were maintained at 37°C with 5% CO_2 in RPMI-1640 from Wisent supplemented with 5% FBS. RAW 264.7 cells were also used for the PM-GFP FCS and FRAP experiments. They were cultured at 37°C in DMEM (Life Technologies, Invitrogen, Carlsbad, CA) supplemented with 10% FBS (Life Technologies), 50 U/ml penicillin, 50 µg/ml streptomycin sulfate, L-glutamine, and 110 mg/ml sodium pyruvate. As recommended by ATCC, CO_2 was maintained at 10% due to the high sodium bicarbonate level of the Life Technologies media used.

Sample preparation

Bodipy-TMR-PIP_2 and TopFluor-PIP_2 were injected into J774a.1 cells in the form of arachidoyl Lyso-PC/fluorescent-PIP_2 micelles as described previously (Golebiewska *et al.*, 2008). The composition of micelles was 82% arachidoyl Lyso-PC and 18% fluorescent-PIP_2. Lipids were suspended in 1 mM EDTA solutions, warmed to 37–42°C, mixed, and diluted with 1 mM EDTA to a concentration of ~500 µM, and then sonicated in a bath sonicator for 3–5 s to form the mixed micelles. We used mixed micelles rather than PIP_2 micelles because PIP_2 micelles aggregate in the presence of the 1 mM Ca^{2+} present in the bathing solution, causing the pipette tips to clog.

$DiIC_{12}$ was dissolved in ethanol and added to cells by mock microinjections (with the Pi and Pc set to 0). The final concentration of ethanol in the cell was <0.01%.

Latex beads were coated with human IgG as previously described (Steinberg and Grinstein, 2009). Briefly, beads were washed three times with phosphate-buffered saline (PBS), incubated with human IgG for 1 h at room temperature, and again washed three times with PBS.

For frustrated phagocytosis measurements, the coverslips were incubated with 1% BSA in PBS at room temperature for 1 h, extensively washed in PBS, and then incubated with PBS containing 10 µg/ml mouse anti-BSA antibody for ≥1 h at room temperature. After three washes with PBS the coverslips were left in PBS (to prevent drying) until they were moved to the microscope.

Microinjection

Two days before the microinjection experiments, cells were plated in glass bottom MatTek dishes that were marked with a diamond knife (to aid in locating microinjected cells). Needles were pulled on the Flaming Brown instrument using the following settings: heat 780, pull 15, velocity 13, time 20. These needles had slightly larger tips than the commercially available needles from Eppendorf to minimize clogging of the tips. For microinjections we used InjectMan NI2 with FemtoJet pump from Eppendorf (Hauppauge, NY). PIP_2 micelles were microinjected in the cytoplasm. For FCS measurements we set the injection pressure Pi at 17–25 hPa and kept the compensation pressure Pc at 0 (to avoid leakage of PIP_2 micelles from the needle into the bathing solution). For FRAP measurements Pi was set to 35–55 hPa. The injection time was set to 0.4 s for FCS measurements and to 0.6 s for FRAP measurements. Prior to the microinjections we replaced the medium bathing the cells with phenol-free Liebovitz's 15 (L15) medium.

We typically injected ~10 cells in a 10-min period. Microinjections were performed on a Zeiss (Jena, Germany) Axiovert 200M microscope equipped with a 40× long-distance phase 2 objective. We examined the microinjected cells using the phase 2 and epifluorescence to select cells that were both viable and contained a suitable level of fluorescent PIP_2.

We then transferred the cells to the FCS microscope. We measured the diffusion of fluorescent molecules in the plasma membrane of macrophages 10–30 min after microinjection. For the measurements in the phagosomal cup we exposed cells to 8-µm-diameter latex beads coated with human IgG. We examined the cells using both transmitted light and laser scanning function. We placed the FCS focus on the top portion of the membrane enveloping a bead that was at the early stage of phagocytosis.

FCS measurements

As reviewed in detail elsewhere, FCS allows one to measure the fluorescence as a function of time and determine the correlation time, which may be considered as the average time for a single PIP_2 to diffuse out of the confocal area on the plasma membrane illuminated by laser (Elson and Rigler, 2001; Haustein and Schwille, 2007). As the width of the illuminated spot can be determined experimentally, the diffusion coefficient, D, can be determined from the Einstein relation.

Confocal imaging, FCS, and FRAP measurements were performed on a Zeiss LSM 510 Meta/Confocor 2 apparatus and a Zeiss Confocor 3 using standard configurations. Minimal laser powers were chosen to avoid photobleaching of the fluorescent probes. We used a 40× numerical apperture–1.2 C-Apochromat water immersion objective and adjusted the pinholes of the Confocor 2 daily. For FCS measurements of PIP_2 diffusion, we excited Bodipy-TMR-PIP_2 with the 543-nm HeNe laser and collected emission spectra through a 560 LP filter.

To calibrate the effective radius of the detection volume of the Confocor 2 we measured the correlation time of rhodamine ($D = 420\ \mu m^2/s$) in L15 medium and used the Einstein relation, Eq. 2. The effective radius of the detection volume for the 543-nm line was $\omega_1 = 0.22 \pm 0.01$ µm. In our previous work we assumed that rhodamine diffuses with $D = 300\ \mu m^2/s$. To compare our previous measurements with our current results we recalculated the D of PIP_2 in the plasma membrane ($0.8\ \mu m^2/s$; Golebiewska *et al.*, 2008) and obtained the slightly larger value of $D = 1.2\ \mu m^2/s$.

To calculate the effective radius of the confocal volume of the Confocor 3, we measured the correlation time τ_d of several fluorescent dyes with known diffusion coefficients (D) (Ruttinger *et al.*, 2008). We used fluorescein with $D = 436\ \mu m^2/s$ (at 23°C) to calibrate the 488-nm laser line and TMR with $D = 420\ \mu m^2/s$ (at 23°C) to calibrate the 543-nm laser line (Petrasek and Schwille, 2008). The FCS measurements yield $\tau_d = 37 \pm 1$ µs for fluorescein and 38 ± 1 µs for TMR with laser powers of 10 µW and pinhole sizes of 1 airy unit. The effective radius (ω_1) under these conditions is thus 0.25 µm for both the 488-nm and 543-nm laser lines, as calculated from Eq. 2.

We monitored the count rate during data acquisition and rejected measurements with either a substantial increase or decrease in light intensity to avoid artifacts due to either membrane movements or bleaching.

Autocorrelation curves were fitted to the model equation for free Brownian diffusion in two dimensions:

$$G(\tau) = \frac{1}{N} \cdot \frac{1}{1+(\tau / \tau_d)} \quad (1)$$

where N is the average number of particles in the confocal volume and τ_d is the average residence time in the confocal volume. We used software from both SigmaPlot (Systat, San Jose, CA) and Zeiss, employing a least squares algorithm to fit Eq. 1 to the data.

We then obtained the diffusion coefficient, D, from

$$D = \frac{\omega_1^2}{4\tau_d} \quad (2)$$

where ω_1 is the radius of the detection volume and τ_d is the correlation time. For cases with populations of molecules diffusing with different diffusion coefficients but with the same fluorescence quantum yields the equation becomes

$$G(\tau) = \frac{1}{N} \cdot \sum_i \frac{Y_i}{1+(\tau / \tau_{d,i})} \quad (3)$$

where N is the number of molecules and Y_i is the fraction of molecules diffusing with a diffusion coefficient D_i and a correlation time $\tau_{d,i}$. To minimize hydrolysis of PIP_2 after microinjection, all measurements using the Confocor 2 were performed at room temperature, 25 ± 1°C, which was monitored throughout the experiment using a thermocouple. The FRAP measurements on PIP_2 with the Confocor 3 were conducted at room temperature, ~23°C. The FRAP measurements of PM-GFP made on the Confocor 3 were conducted at 37°C.

FRAP measurements

TopFluor-PIP$_2$. To monitor the fluorescence produced by TopFluor-PIP_2, we excited using 1% intensity of the 488-nm line from the argon laser; we recorded images using a 505 LP filter. The scan speed was set to 1.6 µs/pixel, resulting in ~900 ms/frame. The desired area (4–10 µm^2 around a bead that was engulfed 10–50% or the same area on the membrane outside the phagosome) was bleached with 4–10 scans with 100% intensity of the 488-nm line from the argon-ion laser. Typically, as shown in Figure 3, A–D, we recorded three images prior to bleaching and 97 images postbleach with 1-s intervals. The success rate of these experiments was very low. For example, the cells were often damaged upon microinjection of the high concentration of PIP_2; we did not succeed in rapidly bleaching most of the TopFluor-PIP2 in the cup; and the bead moved during the 100 s we followed the recovery. TopFluor-PIP_2 was superior for the FRAP experiments because it bleached more readily; Bodipy-TMR-PIP_2 was superior for the FCS experiments because it did not bleach as easily and for other reasons discussed elsewhere (Golebiewska *et al*., 2008).

We excited $DiIC_{12}$ with the 546-nm line of the HeNe laser and recorded images using a 560 LP emission filter. To bleach $DiIC_{12}$ we used full power of the 488-nm line of the argon-ion laser.

We analyzed the FRAP images using ImageJ or Fiji software and fitted the intensity curves using SigmaPlot.

PM-GFP. RAW macrophages were transfected with either palmitoylated/myristoylated PM-GFP (derived from the N-terminal region of Lyn kinase; see Corbett-Nelson *et al*., 2006) or PMT-GFP (derived from a different protein [Liu *et al*., 2007], a kind gift of Thorsten Wohland). We used the Neon electroporation system (Invitrogen). The 8-µm-diameter latex beads (Bangs Labs) were opsonized with IgG (Sigma-Aldrich) and introduced to the cells bathed in phenol-free L15 medium and incubated at 37°C on the microscope stage. For FRAP, measurements were taken using an LSM 710 confocal microscope (Zeiss), employing the argon-ion 488-nm line to excite fluorescence, and emission longer than 500 nm was collected. Bleaching was performed with 100% power (700 µW), with up to 10 images acquired before and 90 after.

FRAP of RAW macrophages undergoing frustrated phagocytosis was performed on a WaveFX spinning disk microscopy system (Quorum Technologies, Guelph, ON, Canada) equipped with a Mosaic digital diaphragm for photobleaching and operated with the software Volocity, version 4.4 (PerkinElmer, Waltham, MA). Macrophages for frustrated phagocytosis were lightly scraped to lift them from the growth flask, resuspended in RPMI with 25 mM 4-(2-hydroxyethyl)-1-piperazineethanesulfonic acid, and added to coverslips coated with IgG in a heated chamber on the microscope. Cells were allowed to settle by gravity onto the coverslip; when mCherry-actin was observed to form a ring at the beginning of frustrated phagocytosis, FRAP of the coexpressed GFP-tagged protein was performed.

ACKNOWLEDGMENTS

We thank William Trimble for extensive helpful discussions about septin filaments; Xianke Shi for calibration of the Confocor 3; the Mechanobiology Institute at the National University of Singapore for financial support (S.M. and T.M.); the National Institutes of Health for Grant GM053132 (S.S.); and the Intramural Research Program of the National Heart, Lung and Blood Institute, National Institutes of Health (R.W.P.).

REFERENCES

Aoyagi K, Sugaya T, Umeda M, Yamamoto S, Terakawa S, Takahashi M (2005). The activation of exocytotic sites by the formation of phosphatidylinositol 4,5-bisphosphate microdomains at syntaxin clusters. J Biol Chem 280, 17346–17352.

Araki N, Johnson MT, Swanson JA (1996). A role for phosphoinositide 3-kinase in the completion of macropinocytosis and phagocytosis in macrophages. J Cell Biol 135, 1249–1260.

Barral Y, Mermall V, Mooseker MS, Snyder M (2000). Compartmentalization of the cell cortex by septins is required for maintenance of cell polarity in yeast. Mol Cell 5, 841–851.

Botelho RJ, Teruel M, Dierckman R, Anderson R, Wells A, York JD, Meyer T, Grinstein S (2000). Localized biphasic changes in phosphatidylinositol-4,5-bisphosphate at sites of phagocytosis. J Cell Biol 151, 1353–1367.

Coppolino MG, Dierckman R, Loijen J, Collins RF, Pouladi M, Jongstra-Bilen J, Schreiber AD, Trimble WS, Anderson R, Grinstein S (2002). Inhibition of phosphatidylinositol-4-phosphate 5-kinase Iα impairs localized actin remodeling and suppresses phagocytosis. J Biol Chem 277, 43849–43875.

Corbett-Nelson EF, Mason D, Marshall JG, Collette Y, Grinstein S (2006). Signaling-dependent immobilization of acylated proteins in the inner monolayer of the plasma membrane. J Cell Biol 174, 255–265.

Cougoule C, Wiedemann A, Lim J, Caron E (2004). Phagocytosis, an alternative model system for the study of cell adhesion. Semin Cell Dev Biol 15, 679–689.

Di Paolo G, De Camilli P (2006). Phosphoinositides in cell regulation and membrane dynamics. Nature 433, 651–657.

Doughman RL, Firestone AJ, Anderson RA (2003). Phosphatidylinositol phosphate kinases put $PI4,5P_2$ in its place. J Membrane Biol 194, 77–89.

Elson EL, Rigler R (2001). Fluorescence Correlation Spectroscopy. Theory and Applications, Berlin: Springer-Verlag.

Emoto K, Inadome H, Kanaho Y, Narumiya S, Umeda M (2005). Local change in phospholipid composition at the cleavage furrow is essential for completion of cytokinesis. J Biol Chem 280, 37901–37907.

Estey MP, Kim MS, Trimble WS (2011). Septins. Curr Biol 21, R384–R387.

Faty M, Fink M, Barral Y (2002). Septins: a ring to part mother and daughter. Curr Genet 41, 123–131.
Field SJ, Madson N, Kerr ML, Galbraith KAA, Kennedy CE, Tahiliani M, Wilkins A, Cantley LC (2005). PtdIns(4,5)P2 functions at the cleavage furrow during cytokinesis. Curr Biol 15, 1407–1412.
Finger FP (2005). Reining in cytokinesis with a septin corral. Bioessays 27, 5–8.
Froese CD, Trimble WS (2008). The functions of septins in mammals. In: The Septins, eds. PA Hall, SE Hilary Russell, JR Pringle, Chichester, United Kingdom: John Wiley & Sons, 187–210.
Fujita A, Cheng J, Tauchi-Sato K, Takenawa T, Fujimoto T (2009). A distinct pool of phosphatidylinositol 4,5-bisphosphate in caveolae revealed by a nanoscale labeling technique. Proc Natl Acad Sci USA 106, 9256–9261.
Gambhir A, Hangyas-Mihalyne G, Zaitseva I, Cafiso DS, Wang J, Murray D, Pentyala SN, Smith SO, McLaughlin S (2004). Electrostatic sequestration of PIP_2 on phospholipid membranes by basic/aromatic regions of proteins. Biophys J 86, 2188–2207.
Garrenton LS, Stefan CJ, McMurray MA, Emr SD, Thorner J (2010). Pheromone-induced anisotropy in yeast plasma membrane phosphatidylinositol-4,5-bisphosphate distribution is required for MAPK signaling. Proc Natl Acad Sci USA 107, 11805–11810.
Golebiewska U, Nyako M, Woturski W, Zaitseva I, McLaughlin S (2008). Diffusion coefficient of fluorescent phosphatidylinositol 4,5-bisphosphate (PIP_2) in the plasma membrane of cells. Mol Biol Cell 19, 1663–1669.
Hall PA, Russell SEH, Pringle JR, eds. (2008). The Septins, Chichester, United Kingdom: John Wiley & Sons.
Hammond GRV, Sim Y, Lagnado L, Irvine RF (2009). Reversible binding and rapid diffusion of proteins in complex with inositol lipids serves to coordinate free movement with spatial information. J Cell Biol 184, 297–308.
Haustein E, Schwille P (2007). Fluorescence correlation spectroscopy: novel variations of an established technique. Annu Rev Biophys Biomol Struct 36, 151–169.
Hilgemann DW (2007). Local PIP_2 signals: when, where and how? Pflugers Arch 455, 55–67.
Hinchliffe KA, Ciruela A, Irvine RF (1998). PIPkins1, their substrates and their products: new functions for old enzymes. Biochim Biophys Acta 1436, 87–104.
Huang Y-W, Yan M, Collins RF, DiCiccio JE, Grinstein S, Trimble WS (2008). Mammalian septins are required for phagosome formation. Mol Biol Cell 19, 1717–1726.
James DJ, Khodthong C, Kowalchyk JA, Martin TFJ (2008). Phosphatidylinositol 4,5-bisphosphate regulates SNARE-dependent membrane fusion. J Cell Biol 182, 355–366.
Kusumi A, Nakada C, Ritchie K, Murase K, Suzuki K, Murakoshi H, Kasai RS, Kondo J, Furiwara T (2005). Paradigm shift of the plasma membrane concept from the two-dimensional continuum fluid to the partitioned fluid: high speed single molecule tracking of membrane molecules. Annu Rev Biophys Biomol Struct 34, 351–378.
Kusumi A, Shirai YM, Koyama-Honda I, Suzuki KGN, Fujiwara TK (2010). Hierarchical organization of the plasma membrane: investigations by single-molecule tracking vs. fluorescence correlation spectroscopy. FEBS Lett 584, 1814–1823.
Lam AD, Tryoen-Toth P, Tsai B, Vitale N, Stuenkel EL (2008). SNARE-catalyzed fusion events are regulated by syntaxin1a-lipid interactions. Mol Biol Cell 19, 485–497.
Lingwood D, Simons K (2010). Lipid rafts as a membrane-organizing principle. Science 327, 46–50.
Liu P, Sudhaharan T, Koh RML, Hwang LC, Ahmed S, Maruyama IN, Wohland T (2007). Investigation of the dimerization of proteins from the epidermal growth factor receptor family by single wavelength fluorescence cross-correlation spectroscopy. Biophys J 93, 684–698.
Mao YS, Yin HL (2007). Regulation of the actin cytoskeleton by phosphatidylinositol 4-phosphate 5 kinases. Pflugers Arch 455, 5–18.
Mao YS *et al*. (2009). Essential and unique roles of PIP5K-γ and -α in Fcγ receptor-mediated phagocytosis. J Cell Biol 184, 281–296.
Marshall JG, Booth JW, Stambolic V, Mak T, Balla T, Schreiber AD, Meyer T, Grinstein S (2001). Restricted accumulation of phosphatidylinositol 3-kinase products in a plasmalemmal subdomain during Fcγ receptor-mediated phagocytosis. J Cell Biol 153, 1369–1380.
McLaughlin S, Murray D (2005). Plasma membrane phosphoinositide organization by membrane electrostatics. Nature 438, 605–611.
McLaughlin S, Wang J, Gambhir A, Murray D (2002). PIP_2 and proteins: interactions, organization and information flow. Annu Rev Biophys Biomol Struct 31, 151–175.
McMurray MA, Thorner J (2009). Septins: molecular partitioning and the generation of cellular asymmetry. Cell Division 4, 18.
Melikyan GB, Deriy BN, Ok DC, Cohen FS (1996). Voltage-dependent translocation of R18 and DiI across lipid bilayers leads to fluorescence changes. Biophys J 71, 2680–2691.
Milosevic I, Sorensen JB, Lang T, Krauss M, Nagy G, Haucke V, Jahn R, Neher E (2005). Plasmalemmal phosphatidylinositol-4,5-bisphosphate level regulates the releasable vesicle pool size in chromaffin cells. J Neurosci 25, 2557–2565.
Morone N, Fujiwara T, Murase K, Kasai R, Ike H, Yuasa S, Usakura J, Kusume A (2006). Three-dimensional reconstruction of the membrane skeleton at the plasma membrane interface by electron tomography. J Cell Biol 174, 851–862.
Oh Y, Bi E (2011). Septin structure and function in yeast and beyond. Trends Cell Biol 21, 141–148.
Petrasek Z, Schwille P (2008). Precise measurement of diffusion coefficients using scanning fluorescence correlation spectroscopy. Biophys J 94, 1437–48.
Raucher D, Stauffer T, Chen W, Shen K, Guo S, York JD, Sheetz MP, Meyer T (2000). Phosphatidylinositol 4,5-bisphosphate functions as a second messenger that regulates cytoskeleton-plasma membrane adhesion. Cell 100, 221–228.
Ruttinger S, Buschmann V, Kramer B, Erdmann R, Macdonald R, Koberling F (2008). Comparison and accuracy of methods to determine the confocal volume for quantitative fluorescence correlation spectroscopy. J Microsc 232, 343–352.
Santarius M, Lee CH, Anderson RA (2006). Supervised membrane swimming: small G-protein lifeguards regulate PIPK signaling and monitor intracellular PtdIns(4,5)P_2 pools. Biochem J 398, 1–13.
Schmidt K, Nichols BJ (2004). A barrier to lateral diffusion in the cleavage furrow of dividing mammalian cells. Curr Biol 14, 1002–1006.
Scott CC, Dobson W, Botelho RJ, Coady-Osberg N, Chavrier P, Knecht DA, Heath C, Stahl P, Grinstein S (2005). Phosphatidylinositol-4,5-bisphosphate hydrolysis directs actin remodeling during phagocytosis. J Cell Biol 169, 139–149.
Sirajuddin M, Farkosovsky M, Hauer F, Kuhlmann D, Macara IG, Weyland M, Stark H, Wittinghofer A (2007). Structural insight into filament formation by mammalian septins. Nature 449, 311–315.
Steinberg BE, Grinstein S (2009). Pathogen destruction versus intracellular survival: the role of lipids as phagosomal fate determinants. In: Methods in Molecular Biology. Macrophages and Dendritic Cells, ed. NE Reiner, New York: Humana Press, 2002–2011.
Stuart LM, Ezekowitz RAB (2005). Phagocytosis: elegant complexity. Immunity 22, 539–550.
Swaney KF, Huang C-H, Devreotes PN (2010). Eukaryotic chemotaxis: a network of signaling pathways controls motility, directional sensing, and polarity. Annu Rev Biophys 39, 365–289.
Swanson JA (2008). Shaping cups into phagosomes and macropinosomes. Nature Rev Mol Cell Biol 9, 639–649.
Takizawa PA, DeRisi JL, Wilhelm JE, Vale RD (2000). Plasma membrane compartmentalization in yeast by messenger RNA transport and a septin diffusion barrier. Science 290, 341–344.
Vasudevan L, Jeromin A, Volpicelli-Daley L, De Camilli P, Holowka D, Baird B (2009). The β- and γ-isoforms of type I PIP5K regulate distinct stages of Ca^{2+} signaling in mast cells. J Cell Sci 122, 2567–2574.
Weernink PAO, Schmidt M, Jakobs KH (2004). Regulation and cellular roles of phosphoinositide 5-kinases. Eur J Pharmacol 500, 87–99.
Wenk MR, Pellegrini L, Klenchin VA, Di Paolo G, Chang S, Daniell L, Arioka M, Martin TF, De Camilli P (2001). PIPkinase Iγ is the major PI(4,5)P_2 synthesizing enzyme at the synapse. Neuron 32, 79–88.
Williams D, Vicogne J, Zaitseva I, McLaughlin S, Pessin JE (2009). Evidence that electrostatic interactions between vesicle-associated membrane protein 2 and acidic phospholipids may modulate the fusion of transport vesicles with the plasma membrane. Mol Biol Cell 20, 4910–4919.
Yeung T, Ozdamar B, Paroutis P, Grinstein S (2006). Lipid metabolism and dynamics during phagocytosis. Curr Opin Cell Biol 18, 429–437.
Yoshida S, Bartolini S, Pellman D (2009). Mechanisms for concentrating Rho1 during cytokinesis. Genes Dev 23, 810–823.